Land Use Policy 109 (2021) 105637

Contents lists available at ScienceDirect

Land Use Policy

journal homepage: www.elsevier.com/locate/landusepol

A topological-based approach for determining spatial relationships of complex volumetric parcels in land administration systems

Ruba Jaljolie [a], Kirsikka Riekkinen [b], Sagi Dalyot [a,*]

[a] Mapping and Geo-Information Engineering, Faculty of Civil and Environmental Engineering Technion – Israel Institute of Technology Technion, Haifa 3200003, Israel
[b] Department of Built Environment, School of Engineering, Aalto University, P.O. Box 12200, 00076, The National Land Survey of Finland, Finland

ARTICLE INFO

Keywords:
Land Administration
3D Cadaster
Volumetric Parcels
Urbanization
Topology

ABSTRACT

Present changes in land property originate from sizable density growth of the urban environment, led by the high demand of land, especially in industrial and commercial centers. This urbanization development - above and below ground - causes an acute need for developing land administration systems to accommodate current and future demands in land management on the one hand, and urban planning perspectives on the other hand. One approach calls for the design of 3D cadastral registration and management systems, which are planned to replace the well-established 2D systems. One of the key processes that these systems should handle for various cadastral workflows, such as parcel insertion and partition, is accurately determining the spatial topological relationship that exist between 3D Volumetric Parcels. These processes are relatively simple to implement between non-complex 3D Volumetric Parcels, but the reality is that the 3D Volumetric Parcels are mostly geometrically complex. In this paper, we suggest methods and processes based on simplifying unbounded, hollowed, curved, and concaved 3D Volumetric Parcels to enable their robust and accurate spatial relationship determination. As part of the comprehensive solution, we propose a subdivision algorithm used for concaved 3D Volumetric Parcels. We have analyzed the various processes on a realistic simulation, proving that the proposed processes were accurate in handling complex 3D Volumetric Parcels by automatically validating their spatial relatioships. We believe that implementing and embedding the developed set of tools in 3D land administration systems is a step forward in the realization of comprehensive land processes that are essential for the automatic management of our complex and developing urbanization.

1. Introduction

The growing density of urban construction and the high demand of land, especially in industrial and commercial centers, lead to the overlap and integration of complex structures in space. Rapid changes in land properties are witnessed, and various authorities and experts require the use of land management systems designed to represent the reality as accurate and updated as possible (Krigsholm et al., 2018). According to the UN,[1] the current world population of 7.3 Billion is expected to reach 8.5 Billion by 2030, and 9.7 Billion in 2050, where 66% are expected to live in urban areas. This urbanization process causes an acute need for new conceptualizations related to land administration.

Cadastres have evolved over centuries, responding to the needs of the surrounding society, such that in addition to their original purpose serving taxation and security of tenure, their functions nowadays include multipurpose tools to support the development of modern societies (Ting and Williamson, 1999). Overall, a cadastral system is never static but rather dynamic, and we should not content ourselves into the current system but be looking for new development possibilities of cadastre and cadastral systems (Krigsholm et al., 2020).

Recent research in land administration focuses on the realization of 3D cadastral systems, mainly from organizational and legal perspectives. Main aspects are given to supporting 3D registration of ownership, and the three Rs - Rights, Responsibilities, and Restrictions (e.g., van Oosterom, 2013). These perspectives continue to evolve, where 4D cadaster systems are being proposed by modelling the 3D digital models at different time instances (Doulamis et al., 2015), whereas 5D cadaster systems aim to incorporate 3D indoor Level Of Detail (LOD) hierarchy modeling (e.g., Kang and Lee, 2014; Kemec et al., 2012). However, technical implementation aspects of 3D cadaster are still limited and

* Corresponding author.
E-mail addresses: sruba93@campus.technion.ac.il (R. Jaljolie), kirsikka.riekkinen@aalto.fi (K. Riekkinen), dalyot@technion.ac.il (S. Dalyot).

[1] https://www.un.org/en/sections/issues-depth/population/ Accessed: December 10, 2020.

https://doi.org/10.1016/j.landusepol.2021.105637
Received 2 February 2021; Received in revised form 20 June 2021; Accepted 24 June 2021
Available online 7 July 2021
0264-8377/

impractical, where uniform specifications and detailed steps for running comprehensive 3D functionalities and processes lack. Though abstract approaches and processes for turning existing 2D land management systems to 3D systems are suggested (Jaljolie et al., 2016, 2018), practical mathematical and topological problems related to realistic 3D analysis are not yet sufficiently solved. The shortcomings of applicable 3D procedures and functionalities remain barriers to adopting 3D cadastral systems. Commonly, the topological relationship of two 3D volumetric parcels (3DVPs) is simplified and determined for typical parcels, meaning that both serve as finite convex parcels that do not include hollows or non-planar surfaces (Bozickovic et al., 2012). However, determining spatial relationships, such as subdivision of two complex 3DVPs, is cardinal for performing basic processes and analysis in 3D land administration systems. For example, the process of inserting a new 3D volumetric parcel in an existing 3D database requires assuring that the new inserted parcel does not overlap existing parcels' three Rs; meaning that the spatial relationships between the newly added parcel and the existing ones should be accurately determined, before actual insertion can take place.

This paper presents practical solutions for the above-mentioned barriers, by providing and developing a set of functionalities to accurately determine the relationship between any given two 3DVPs. The presented solution also handles the implementation of a customized data structure for representing and analyzing the 3DVPs. This paper is structured as follows: Chapter 2 reviews current research on topological relationship analysis of 3D parcels on a larger context, and 3D land administration systems; Chapter 3 describes the methodology and the developed algorithms for determining the spatial relationship between any given two 3DVPs, including the description of the algorithms' shortcomings and possible enhancements (Python pseudocodes of all algorithms are presented in the appendices); Chapter 4 presents an implementation of the developed algorithms, including a simulation of a planned railway tunnel insertion, followed by providing preliminary examination of the resulting legislative steps; Chapter 5 provides a discussion, with summary and outlooks for possible applications that can implement our solution and concludes the study. We believe that the presented set of tools designed specifically for 3D land administration systems is a step forward in the realization of comprehensive land processes that are essential for the automatic management of our complex and developing urbanization. Thus, we may say that the contribution of this study is to add one possible technical solution into the discussion on 3D parcels and cadastre and decrease the gap between institutional and technical discussion on 3D land administration.

2. Literature review

Turning 2D land management systems into 3D systems have been extensively investigated (e.g., Seifert et al., 2017; Doulamis et al., 2015). However, to the best of our knowledge, most operating national cadastral systems in the world are 2D, although examples of conceivable 3D land management systems were discussed (e.g., Kalogianni et al., 2020; Dimopoulou and Van Oosterom, 2019; Van Oosterom, 2018). These studies mostly present prototypes that handle very specific and partial operations necessary for future 3D cadastral systems.

2.1. Geometry and topological relationships of cadastral objects

3D geometry and topological relationships are intensively researched. For example, Shi et al. (2019) employ Conformal Geometric Algebra (CGA) for presenting cadastral data and determining topological relationships between 3D cadastral objects. Authors distinguish among 13 kinds of topological relationships of a cadastral parcel and a boundary point, and 48 spatial relationships of a cadastral parcel and a boundary line. Most solutions employing CGA (e.g., Luo et al., 2017a; Luo et al., 2017b; Zhang et al., 2016; Yu et al., 2016), are based on algebra, algebraic definitions, and algebraic calculations, which are not appropriate for managing hierarchical data structure, thus not enabling performing the subdivision functionality, for example, as we propose here.

Generating 3D objects and detecting topological relationships between 3D parcels - other than CGA - is investigated by Hmida et al. (2013). The authors model the topological relationships between two objects based on a Selective Nef Complexes (SNC) Nef Polyhedra, which is defined as a set of points in D dimensions (3 dimensions in this case) containing open half spaces. Combined with its Boolean operators, SNC enables implementing unary (e.g., interior) and binary Boolean operators (e.g., union and intersection). Only part of these SNC-Boolean operators (namely: intersection, interior, boundary, and complement) are required for creating 9-Intersection Model (9-IM) matrix. Based on the calculated values in the 9-IM matrix, the topological relationship between two objects is determined as one of the Egenhofer Relations (Egenhofer and Franzosa, 1991), which are: Equals, Disjoint, Meet, Overlap, Covers, Covered by, Inside, and Contains. The approach suggested by the authors is based on calculating the boundaries, interiors, and exteriors of existing 3D objects. However, this solution fits only specific types of data structure, while not relying on cartesian coordinates that fits a hierarchical data structure for detecting one of eight possible relationships between two 3D entities – as we propose here.

Ying et al. (2015) suggest a methodology for constructing and distinguishing complex and non-manifold volumetric solids. For generating 3D objects, their approach applies an algorithm for creating solids based on their input faces, with the underlying assumption that the topological relationships (i.e., node, edge, face) on a face are already distinguished. This solution does not detect the exact relationship between two parcels (i.e., one of eight possible relationships according to the Dimensionally Extended 9-IM (DE-9IM): cover, meet, equal, ……). Instead, it outputs whether two 3DVPs share a node, an edge or a face. This is achieved through the creation process of new 3D parcels, based on their input faces, which enables avoiding post validation of existing objects in the database. However, in some cases it is preferable to postpone relationships analysis to the stage after inserting parcels rather than through the insertion process, for accelerating the insertion. For example, when only a limited number of parcels is inserted into the database, and most of the parcels are already built. The algorithm works for regular 3D objects, pyramids and complex objects that may include hollows or are self-touching. However, the assumption that faces are known does not serve further functions, such as subdivision. Among the steps of subdivision, we need to create new faces in the parcels that are the result of the subdivision, and we cannot assume the faces are known. Among the major differences between Hmida et al. (2013) and Ying et al. (2015) is that the approach suggested in the first calculates topological relationships for objects that already exist in the database, while the latter suggests an algorithm for determining topological relationships between objects directly when they are being inserted into a cadastral database.

Another example exists in Chen et al. (2008), implementing a Geo-DBMS based approach, which provides a comparison between geometry and topology data types. Among the main conclusions made by the authors was that the execution time needed to achieve the geometrical data type analysis was significantly higher than the topological data type; this result encourages applying topological-based approaches. Shojaei et al. (2017) suggest and implement four geometric validation rules in 3D digital cadaster. First rule imposes that the outer boundary of newly created parcels (the result of subdivision, for example) should correspond with the outer boundary of the original canceled parcel(s). Second rule verifies that there is no intersection between 3D entities, i.e., 3D parcels do not overlap. Intersection is allowed only in specific defined cases of secondary element (e.g., an easement or a restriction that is not defined as parcel) overlapping other parcels. Third rule guarantees that faces of 3D parcels are all flat (i.e., a principle in boundary representation approach). Fourth rule validates geometric closure. The suggested method is based on two Euler equations, as described in Ericson (2004).

2.2. Data models of cadastral objects

Granados et al. (2003) used Theory of Nef polyhedral data structure for describing n-dimensional entities, suggesting an algorithm for this purpose that is based on the construction of sphere maps, classifications of local neighborhoods, and simplifications in 3D and Boolean operations. The data structure of selective Nef complex was created based on: "edges", "edge uses", "facets", "shells" and "volumes". For performing Boolean operations, namely: boundary, closure, interior, exterior and regularization, Nef polyhedral is represented as a selective Nef complex (SNC) data structure. Two main algorithms were introduced by the authors: Kd-tree for point location and ray shooting and box-intersection algorithm (described in Zomorodian and Edelsbrunner (2000), for finding intersections. This solution, however, does not fit our objective since it is based on Boolean operations.

Congli and Tsuzuki (2004) suggest a data structure that combines the technologies of solid modelling and geometric modelling. The authors suggest two structures: (1) principal data structure; and (2) auxiliary data structure. The first "contains the original solid model with its geometry" and the second "represents an approximation of the solid model". Methods for synchronizing these two data structures were provided, i.e., synchronizing polyhedral approximation to its geometric representation. Bureick et al. (2016) analyzed surfaces and curves approximation based on 3D point clouds, using free-form surfaces in the approximation processes, such as: polynomial function, Bézier and B-Spline functions, and Non-Uniform Rational B-Splines (NURBS). The approximation processes were described along with a mathematical background, showing that free-form curves can be used for almost any sort of approximation. Pigot (1991) also uses a hierarchical approach for presenting topological primitives; this approach prevents inconsistencies and reduces information redundancy. Accordingly, we adopt the hierarchical data structure in our approach.

3. Methodology

3.1. Data model

Since the determination of the spatial location of the vertices composing one parcel are made in relation to the other parcel, a perquisite is that parcels are defined using right hand Cartesian coordinate system to define the axes' direction. Accordingly, each face in the 3DVP is composed of counterclockwise series of edges from the perspective of an observer standing outside the parcel - meaning that the normal of each face points outwards. Parametric mathematical definition is used for storing spatial objects, which enables easy performance of vectors' calculations and mathematical operations, as well as efficient data management (in terms of memory use). The following functions implementation are performed automatically.

As setting the data model for defining 3D objects significantly influences the structure of the functions, we decided to implement a hierarchical data structure to employ our solution, according to the following rules: 3D Node ↔ 3D Line ↔ 3D Face ↔ 3DVP (Fig. 1). This definition allows considering 0D, 1D, and 2D as special cases of the general 3D data (objects). For instance, a 2D line is a 3D line with a constant value of z, which is practical and reliable for managing the integration of 2D and 3D data. This definition is also expected to enable the expanding of the existing cadastral systems uniformly and smoothly from 2D to 3D, while preserving the principles of the 2D systems.

3.2. Relationships of simple 3DVPs

The method proposed in this research for determining the spatial relationship between two complex 3DVPs extends the idea presented in Bozickovic et al. (2012). The authors describe eight possible spatial relationships between two given simple spatial bodies, defined as A and B: (1) *A disjoints B*; (2) *A contains B*; (3) *A is contained by B*; (4) *A is identical to B*; (5) *A touches B*; (6) *A covers B*; (7) *A is covered by B*; and (8) *A overlaps B*. To solve ambiguities and expansive computation resources, the authors define an aggregation of several spatial topologic conditions, which the developed algorithms follow, for identifying the existing spatial relationship. The idea is that the spatial relationship of the 3DVPs can be practically determined according to the relationships between the vertices of both 3DVPs, as presented in Table 1.

The above-mentioned rules work only for simple parcels but fail for complex ones: the last three relationships, namely overlap, meet, and disjoint, cannot be correctly identified according to these rules. It is

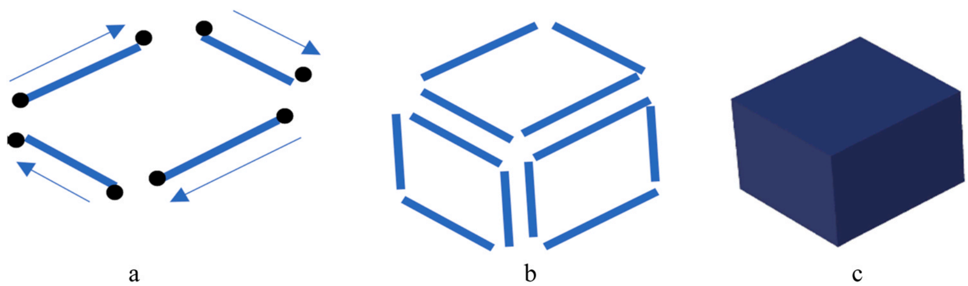

Fig. 1. The employed hierarchical data structure for storing and representing 3DVP: from nodes and lines (a) to faces (b) and 3DVP (c).

Table 1
The spatial topologic rules of two 3DVPs vertices used for defining the existing spatial relationship (source: Bozickovic et al., 2012): ø denotes an Empty group, ¬ø denotes a Not Empty group, and ø/¬ø denotes an Empty/Not Empty group.

	Vertices of A in Relation to B			Vertices of B in Relation to A		
	vertices inside B	vertices outside B	vertices touch B	vertices inside A	vertices outside A	vertices touch A
A inside B	¬ø	ø	ø	ø	¬ø	ø
A contains B	ø	¬ø	ø	¬ø	ø	ø
A equals B	ø	ø	¬ø	ø	ø	¬ø
A covers B	ø	¬ø	¬ø/ø	¬ø/ø	ø	¬ø
A covered by B	¬ø/ø	ø	¬ø	ø	¬ø	¬ø/ø
A overlaps B	¬ø/ø	¬ø	¬ø/ø	¬ø/ø	¬ø	¬ø/ø
A meets B	ø	¬ø	¬ø/ø	ø	¬ø	¬ø/ø
A disjoints B	ø	¬ø	ø	ø	¬ø	ø

required to implement a supplementary examination, which assesses whether an intersection between the 3DVPs' lines and faces exists: (1) if no intersection exists, the relationship is disjoint; (2) if all intersections exist on one face of parcel A and one face of parcel B, the relationship is meet; otherwise, (3) the relationship is overlap. Analyzing the above, we found cases were these does not lead to correct relationship detection, detailed in Section 3.3.

For solving these, we have modified this algorithm: when the relationship of two parcels is none of the first five relations in Table 1, we implement the examination in both directions: once for checking the relationship of the edges in parcel *A* with the faces of parcel *B*, and once for checking the relationship of edges in parcel *B* with the faces of parcel *A*, as follows:

1. If both directions' output is *disjoint*, then the relationship is *disjoint*.
2. If at least one direction output is *meet*, while the other output is either *meet* or *disjoint*, then the relationship is *meet*.
3. If at least one direction output is *overlap*, while the other output is either *overlap* or *disjoint*, then the relationship is *overlap*.

3.3. Relationship of complex 3DVPs

To extend the rudimentary definitions made in Bozickovic et al. (2012), we categorize the possible complex relationship cases into three groups: (1) *partially unbounded*; (2) *concave* or *hollowed*; (3) *non-parallel roof/front*. We provide a textual definition and description for each group, present why the basic approach fails, and present our approach to overcome it. For dealing with concave parcels, we also provide an algorithm for subdividing concave parcels (Section 3.4), which can be also applied for hollowed parcels.

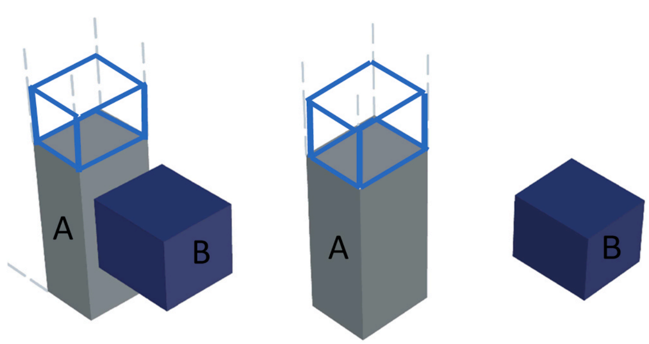

Fig. 2. A schematic example of an unbounded parcel *A* that *meets* a bounded parcel *B* (left), and an unbounded parcel *A* that *disjoints* a bounded parcel *B* (right). For both cases, an artificial face (roof) is generated for parcel *A* (transparent box) that relies on the vertices value of parcel *B*.

3.3.1. Partially unbounded parcels

The basic approach for identifying the spatial relationship between two 3DVPs, defined as *A* and *B*, is based on the faces' normal. Accordingly, the finite values of the vertices of each parcel are fundamental to carry out the relationship analysis. In the cadastral context, a volumetric parcel is fully bounded in all dimensions, while unbounded parcels are parcels with no top or bottom faces and vertices, representing 2D footprints that include the air column above - or below (Thompson and van Oosterom, 2011). Thus, the basic approach will fail here. In the case that only one parcel is unbounded (let it be parcel *A*), it can be perceived that three relationships cannot exist: (1) *A* is *inside B; (2) A* is *covered* by *B;* and (3) *A equals to B*.

To solve this, we create artificial temporary boundaries in unbounded parcels prior to running the analysis. Artificial boundaries are created according to two criteria, whereas the boundaries of parcel *A* must be: (1) higher than the highest vertex of parcel *B*; and (2) higher than parcel's *A* floor (i.e., the generated artificial roof is higher than the original floor). This is automatically implemented by adding a spatial buffer to the largest height value among the two criteria, schematically depicted in Fig. 2. The same applies if parcel *A* is open to the ground: its artificial boundaries must be lower than the lowest vertex of parcel *B*, and lower than parcel's *A* roof.

3.3.2. Concave and hollowed parcels

Applying the basic approach when at least one parcel is hollowed would lead to correct results only if the relationship between the two parcels is either *disjoint*, *overlap* or *meet*. This is since when at least one parcel is hollowed, it is impossible to detect the location of the other parcel's vertices relatively to the hollowed parcel since the normal of a face may intersect other faces in the parcel. Dealing with this ambiguity, we suggest a subdivision algorithm (described in Chapter 3.4 for handling hollowed parcels). Another solution, depicted in Fig. 3, is to geometrically 'fix' the hollowed parcel geometry, and thus instead of checking the relationship between parcel's *B* vertices and parcel *A*, we replace the original hollowed parcel *A* with: (1) an inner parcel (denoted by *A2*) that delimitates the hollow volume of A; and (2) an outer parcel (denoted by *A1*) that delimitates the volume of the original parcel *A* combined with the volume of the hollow (i.e., *A1* is a combination of *A* and *A2*, where *A1* has no hollow), i.e., *A*=*A1*-*A2*. Accordingly, we check all possible relationships of any vertex *p* in parcel *B* with parcels *A1* and *A2*, depicted in Eq. (1).

$$\begin{aligned} p &\in \delta A1 \wedge p \in A2^{-} \Rightarrow p \in \delta A \\ p &\in A2edges \Rightarrow p \in \delta A \\ p &\in A1^{-} \vee p \in A2^{\circ} \Rightarrow p \in A^{-} \\ p &\in \delta A1 \wedge p \in \delta A2 \wedge p \notin A2edges \Rightarrow p \in A^{-} \\ p &\in A1^{\circ} \wedge p \in A2^{-} \Rightarrow p \in A^{\circ} \end{aligned} \tag{1}$$

3.3.3. Parcels with non-planar surfaces (curves)

For detecting the location of a vertex in parcel *B* relatively to parcel

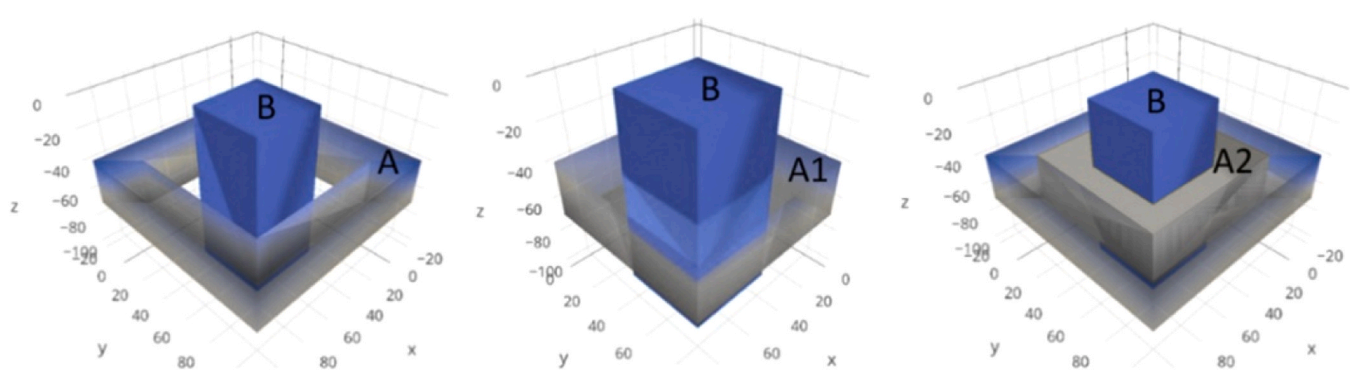

Fig. 3. A schematic example of a hollowed parcel *A* (left). An outer parcel *A1* delimitating the volume of the original parcel *A* and the hollow (middle). An inner parcel *A2* delimitating only the volume of the hollow inside parcel *A* (right).

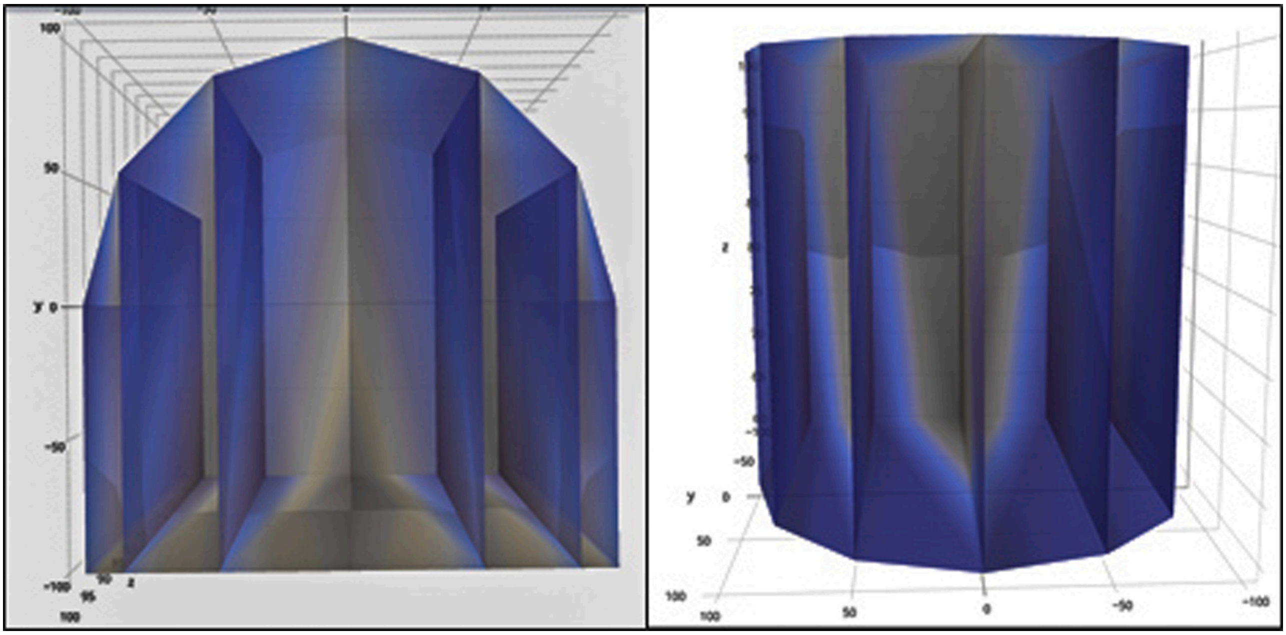

Fig. 4. A schematic example of an approximation of a curved surface: side view (left) and top view (right).

A, the basic approach relies on substituting the vertex coordinates into planar surface equation. In the case that the parcel's surface is not planar, the basic approach will fail since the curved surface analytic representation is unknown; thus, the relationship of this face and the vertices defining another parcel cannot be determined. For solving this problem, an analytic representation for a non-planar surface should be provided. Still, this is not always possible, since parametric equations are available only for finite sorts of spatial surfaces, such as ellipsoid. Therefore, we suggest replacing one curved surface with several finite planar surfaces, as depicted in Fig. 4. The result is a district representation (approximation) of a continuous surface, such that as the number of the replacing surfaces increases, the relationship result will be more accurate and closer to the reality.

Following the notion of Karki et al. (2013): "From a database storage and geometrical validation perspective, curved surfaces can be represented as polyhedral surfaces with planar faces, but this must be recognized as an approximation and not the legal definition". Accordingly, several approximation methods can be followed. If, for example, the surface has a circular cross-section, then we can mathematically calculate the coordinates of several points on its circumference. This applies for other surface types, which can be algebraically or parametrically described, such as an ellipse. This form of approximation requires surfaces with known formula. However, there are cases where the formula describing the surface is unknown and dealing with such problems can rely on the Simpson-based approximation methods or a polynomial approximation. For practicality reasons, if the coordinates of a cadastral object were calculated in the planning stages, and measured for validation in as-made stages, then the calculated or measured coordinates might be entered to the system and used for approximating the curved faces. Point cloud attitude might also be followed: if the 3D geometry of a cadastral object was extruded from a measured point cloud, then the coordinates of the original points, after filtering and noise cleaning, might be used for the approximation process.

3.4. Subdivision function

Using a subdivision function is frequently suggested in the literature as a solution for dealing with 3D parcels that are concave. However, this function is rarely implemented, nor an algorithm for its implementation is provided. The approach described in Section 3.1 does not work for concave (or hollowed) parcels due to the complexity of correctly determining the location of a vertex relatively to concave (or hollowed) parcels. If such a parcel is subdivided into convex sub-parcels, then, its relationship to any vertex should be detected based on the relationship of its sub-parcels to that vertex (see 3.4.3). Here, we suggest an automated approach for geometric subdivision, defined as "Subdivision Function". For presenting the algorithm, we define the terms we use, declare the input and output, provide an example, and explain the different steps.

3.4.1. Terms

- "*convex*": the definition of a 3D parcel that includes no hollows, and the normal to its faces do not converge. A "*convex*" has no dents or cavities and passing a line through a "*convex*" intersects only two faces.

  Condition 1: Let $F \in \mathbb{R}^3$ and $V \in \mathbb{R}^3$ be the faces and vertices of a 3DVP, respectively. $P \in \mathbb{R}^3$ is a convex parcel if $\forall f \in F{:}\overrightarrow{n_f} = \{A\ B, C\}$, where $v1_t = (x1_t, y1_t z1_t)$ and $v1_f = (x1_f, y1_f, z1_f)$ are terminal and start vertices of any edge on f $\forall v \in V, \langle \overrightarrow{n_f}, v - v1_t \rangle \geq 0 \vee \forall v \in V, \langle \overrightarrow{n_f}, v - v1_t \rangle \leq 0$
- "*concave*": the definition of a 3D parcel with hollow, or any 3D parcel in which the normals to its faces converge. A "*concave*" parcel has dent or cavity and passing a line through a "*concave*" might intersect more than two faces. If Condition 1 is not fulfilled, then the parcel is "*concave*".
- "*Subdividing face*": an original face of the original concave parcel that was stretched to be used for subdividing the original parcel into two sub-parcels (Fig. 5 middle). This is a face that defines the limits where a concave parcel would be subdivided for extracting its sub-parcels. For a face to be selected as a "*subdividing face*", it should fulfill the condition that the original vertices of the original parcel exist on both sides, i.e., some of the original parcel vertices are located on its right side, while other vertices exist on its left side. This condition guarantees that the parcel is concave and needs to be subdivided.

  For a "*subdividing face*" - "*sf*" in parcel P:

  Condition 2: If there is $v_k \in V, \langle \overrightarrow{n_f}, v_k - v1_t \rangle > 0$ there must be $v_j \in V, \langle \overrightarrow{n_f}, v_j - v1_t \rangle < 0$

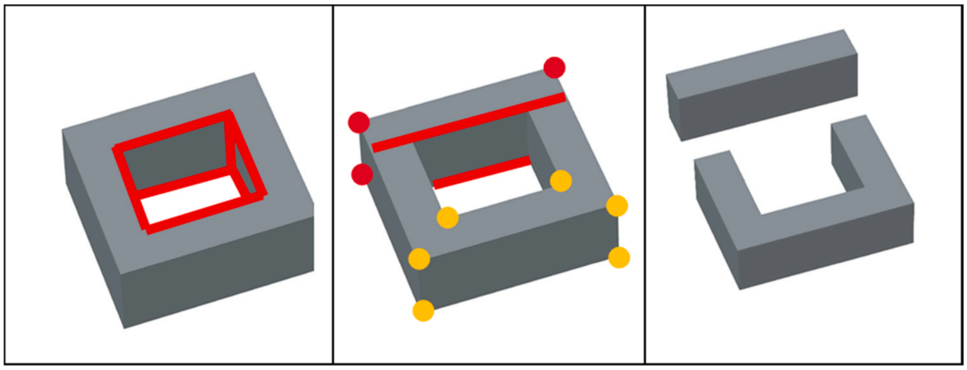

Fig. 5. Faces with "*subdivision*" flag set to "1" appears in red (left). Arbitrary chosen subdividing face appears in red (middle). Two sub-parcels created in the first iteration of the process (right).

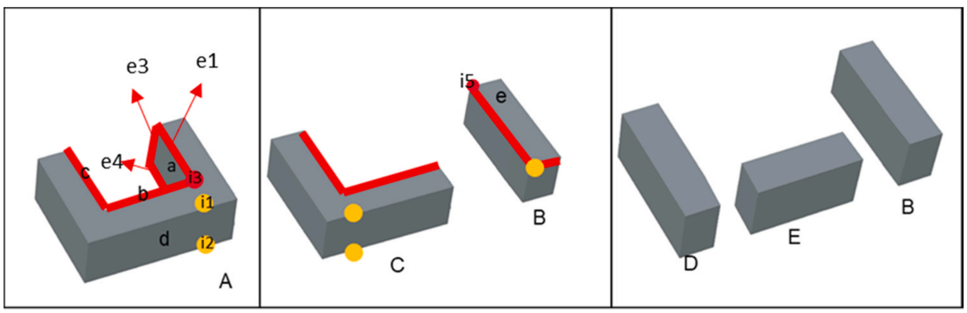

Fig. 6. A schematic example of the subdivision function: parcel *A* (left) is subdivided into two sub-parcels *C* and *B* (middle), and sub-parcel *C* is subdivided into two sub-parcels *D* and *E* (right).

- "*Stretched subdividing face*": a "*subdividing face*" after being stretched.
- "*Sub_left*": a sub-parcel resulting by subdividing the original parcel, left-sided relatively to "*subdividing face*".
  Condition 3: $\forall v \in V, \langle \overrightarrow{n_f}, v - v1_t \rangle \leq 0$
- "*Sub_right*": a sub-parcel resulting by subdividing the original parcel, right-sided relatively to "*subdividing face*".
  Condition 4: $\forall v \in V, \langle \overrightarrow{n_f}, v - v1_t \rangle \geq 0$
- "*Intersection points*": these are the vertices constituting the "*stretched subdividing face*". For stretching the original "*subdividing face*", and defining its new (stretched) limits, its new vertices - "*intersection points*" - should be declared (Fig. 5 middle).
- Condition 5: let $v_i = x_i, y_i, z_i \in \mathbb{R}^3$represent an "*intersection point*" where $\overrightarrow{n_{f_s}} = A_{f_s}, B_{f_s}, C_{f_s}$ is the normal of the "*subdividing face*", then: $A_{f_s}x_i + B_{f_s}y_i + C_{f_s}z_i = D_{f_s}$ and $\forall e_{f_s} \in E, v_i \notin [v_f, v_t]$ where the range of edge is $[v_f, v_t]$.
- "*Other faces*": all the faces in the original concave parcel that were not selected as a "*subdividing face*". "*Intersection points*" are found by intersecting the "*subdividing face*" with all "*other faces*".

3.4.2. Subdivision methodology

The input of this function is a 3DVP, which might be either a concave or a convex. If the input parcel is convex, there is no need to subdivide it, and in this case the "*Subdivision Function*" terminates and returns the original input parcel. If the input parcel is concave, it would be subdivided into two sub-parcels: "*Sub_left*" and "*Sub_right*". The "*Subdivision Function*" is recursive, and if needed it will be implemented again for "*Sub_left*" and for "*Sub_right*". After implementing the "*Subdivision Function*", we receive the convex parcels that constitute the input concave parcel.

The subdivision process constitutes of these stages:

1) Detecting and defining a "*subdividing face*".
2) Finding the "*intersection points*" between a "*subdividing face*" and "*other faces*".
3) Creating a "*stretched subdividing face*" by stretching the subdividing face according to the "*intersection points*".
4) Creating the sub-parcels of a concave parcel, i.e., creating the "*sub_left*" and "*sub_right*" faces.
5) Redo stages 1–4 for "*sub_left*" and "*sub_right*" (i.e., subdivide them again if they are concaves).

The function is illustrated using the example depicted in Fig. 5. Implementing the subdivision algorithm on the parcel on the left will result, in its first step, in two sub-parcels depicted on the right. One of these parcels is convex, and will not be divided again, while the other is concave and must be divided again (Fig. 6).

Parcel *A* (Fig. 6, left) is concave, and should be subdivided. For that, we search a "*subdividing face*", and induce that 3 faces of *A* could be used: face a, b, and c (marked in red in Fig. 6, left). One of these faces would be arbitrary defined as a "*subdividing face*", and parcel *A* is subdivided into two sub-parcels (parcels *B* and *C* in the middle). After that, the left sub-parcel (parcel *C*) is subdivided again into two sub-parcels *D* and *E*. At the end of the subdivision process, 3 sub-parcels are output: *B*, *D* and *E*, which are all convex (Fig. 6, right). More details on the subdivision function are given in Appendix A.

3.4.3. Relationship determination

Following subdividing concave parcel *A*, its relationship with any parcel (denoted by *F*) is detected by checking the location of *F*'s vertices relatively to the sub-parcels of *A*: *B*, *D* and *E* - instead of checking the relationship with *A*. These are described in Fig. 7 and Eq. (2), which outline the tests conducted for determining p^* location relatively to concave parcel *A*, according to its sub-parcels *B*, *D*, and *E*. Based on the output location of vertex p^* relatively to sub-parcels *B*, *D* and *E*, p^* relationship with parcel *A* is detected. Only then, the relationship of *A* and *F* can be inferred.

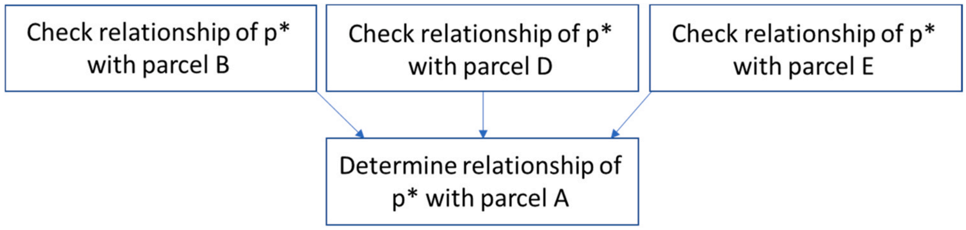

Fig. 7. Determining the relationship of vertex p^* in parcel F and parcel A is based on the vertex's relationship with parcels B, D and E.

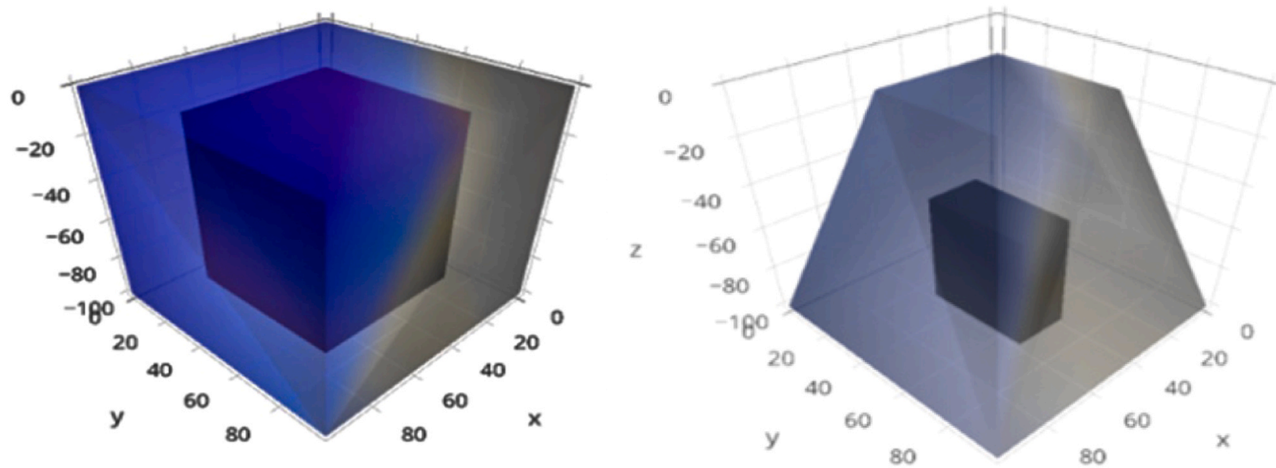

Fig. 8. Validation results for mixed use: *Inside/contain* (left) and *cover/covered* (right).

$$
\begin{array}{l}
\textit{if}\ \ p \in B^- \wedge p \in D^- \wedge p \in E^- \Rightarrow p \in A^- \\
\textit{elif}\ \ p \in B^{\circ} \vee p \in D^{\circ} \vee p \in E^{\circ} \Rightarrow p \in A^{\circ} \\
\textit{elif}\ \ p \in \delta B \wedge p \in D^- \wedge p \in E^- \Rightarrow p \in \delta A \\
\textit{elif}\ \ p \in B^- \wedge p \in \delta D \wedge p \in E^- \Rightarrow p \in \delta A \\
\textit{elif}\ \ p \in B^- \wedge p \in D^- \wedge p \in \delta E \Rightarrow p \in \delta A \\
\textit{elif}\ \ p \in Bedges \vee p \in Dedges \wedge p \in Eedges \Rightarrow p \in \delta A \\
\textit{else}\ \ p \in A^{\circ}
\end{array} \tag{2}
$$

4. Experimental results

All developed functions are programmed in python, together with a simplified GUI used for: (1) uploading the files representing the various 3DVPs; (2) carrying out the relation analysis and evaluation; and (3) visualizing the results. The 3DVPs visualization is carried out using Plotly[2], which provides a robust 3D visualization tool. We examine the developments on fundamental 3D objects (Section 4.1), as well as on a cadastral simulation (Section 4.2).

4.1. Function evaluation

We have tested and analyzed our proposed algorithms and implementation on several fundamental case studies that simulate real cadastral 3DVPs handled in 3D land administration systems. The first example simulates the mixing of public land use into private properties that is very relevant today in urban planning and design (e.g., Hoppenbrouwer and Louw, 2005; Kusumastuti and Nicholson, 2018; Siemiatycki, 2015; Schwanke, 2005), leading to situations where a building is partially owned by a public authority and partially owned by private individuals. Fig. 8 simulates such a case, depicting a "vertical allocation", a term used in Mualam et al. (2019) to describe cases where a part of a private building might be expropriated by the municipality for public use in densely built areas. The algorithm succeeded in detecting the right relationship between a parcel under public authority *contained* (left) in a private parcel or *covered* (right) by it.

The second example (Fig. 9 left) describes an easement, which is the right to benefit from a property of others for a specific reason without possessing it and without the consent of its owners. Fig. 9 left presents a hollowed object (grey) that *meets* another parcel (blue), as identified by our implementation. The grey object represents a hollowed easement that is surrounding the blue parcel, which is partially aboveground and partially underground (under the easement). It should be noted that in this case the subdivision algorithm is implemented on the grey parcel since Bozickovic et al. (2012) does not work for concave parcels. This case can be alternatively solved by the algorithm suggested in Section 3.3.2 for hollowed parcels. Fig. 9 right depicts overlapping parcels (the grey parcel has no holes and it is a convex 3D rectangular parcel that intersects the blue parcel), simulating, for example, a real-world case where a highway cuts through a building (e.g., Osaka, Japan[3]). In this case, the algorithm proposed by Bozickovic et al. (2012) fails: its output will show a *disjoint* relationship because no intersection exists between one parcels' edges and the other parcels' face. None of the eight edges of the grey parcel intersects any face of the blue parcel, leading to the wrong output that the two parcels *disjoint* while they in fact *overlap*. From the other side, the edges of the blue parcel do intersect the faces of the grey parcel and running the algorithm in the opposite direction will output the correct result of *overlap*. The solution we applied for receiving the correct result was stated in Section 3.2.

Meeting relationship might also describe buildings in cities that are subdivided by a border of two countries, such as the city of Baarle-Hertog, where the borderline between Belgium and The Netherlands passes, resulting in houses that partially belong to both countries, e.g.,

[2] https://plot.ly/

[3] https://en.wikipedia.org/wiki/Gate_Tower_Building. Accessed: December 10, 2020.

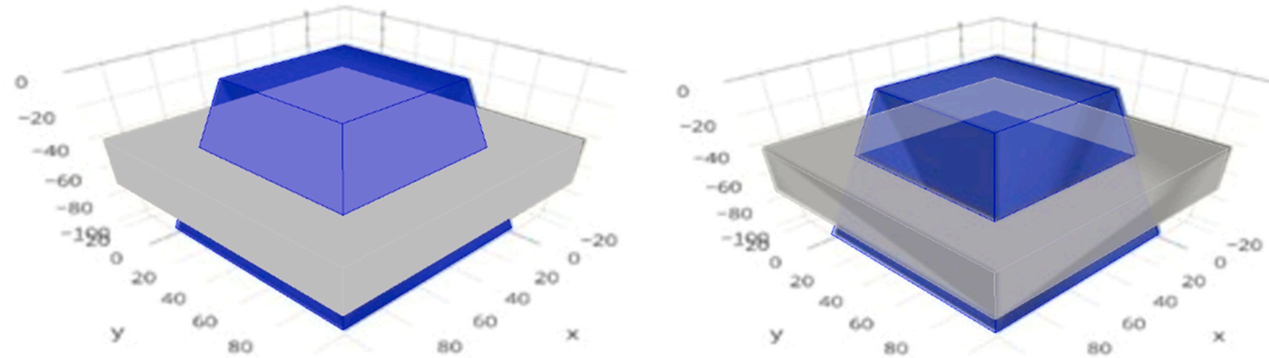

Fig. 9. Validation results for hollowed parcel, showing *meet* relation (left). Validation results for convex parcels, showing *overlap* relation (right).

representing the basic case of neighboring properties, depicted in Fig. 10: none of the blue parcel edges intersect the bottom of the grey parcel, while the edges of grey parcels do intersect the top of the blue parcel. The algorithm correctly detected the relationship after the modification we suggested in chapter Section 3.2.1 - *meet* relationship.

To sum, for all examples presented here the automatic implementation resulted in a correct definition of the spatial relationship that exists between the 3DVPs used for evaluation, as opposed to the basic approach, explained in Section 3.1, that would either fail or produce incorrect results.

4.2. Cadastral simulation

A synthetic 3D model that describes the current state of an area containing 3DVPs above and below the terrain was created in AutoCAD, depicted in Fig. 11. The simulation suggests a scenario, in which a railway tunnel, denoted as a pink cylinder, is planned for construction below the terrain in the specified neighborhood area. It should be noted that our premise is based on the expanding of existing 2D cadaster systems into a 3D one, such that we defined that any existing 2D parcel includes the volume above and beneath its extent (the total air-column). This assumption is valid unless a 3D volume was previously clipped from the air-column, and a 3DVP - including the clipped volume - was created from an expropriation, property transfer, sale or initiating any other cadastral-related transaction. This means that wherever a 3D volumetric parcel exists, a previous vertical division was made.

At the stage of the administrative planning of the railway tunnel, it is necessary to determine the three Rs. For that we check:

1. Whether the planned railway tunnel (or its safety distance range) overlaps other 3DVPs in the area. If yes, then there is a need to (entirely or partially) expropriate the overlapping 3DVP, transfer ownership, and compensate the original owners. If the tunnel overlaps any existing structure, then it may be required to consider changing its route. If it does not overlap any 3DVPs or objects (i.e., no 3DVPs were created earlier in the area), then we check:
2. Which 2D parcels the planned railway tunnel passes under, and accordingly, the 3D volume should be clipped and expropriated from the whole air column delimitating these 2D parcels for the purpose of creating new corresponding 3DVP; accordingly, the original owners of the 2D parcels should be compensated in relation to these new 3DVPs.

The simulation includes 15 parcels, which are defined as 3DVPs

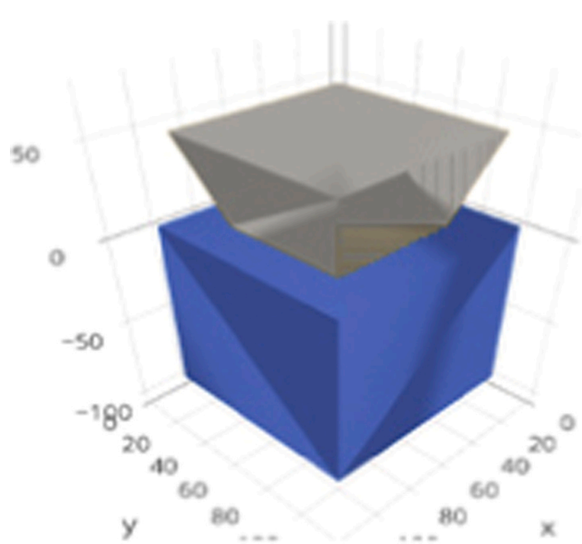

Fig. 10. Validation results for *meeting* parcels.

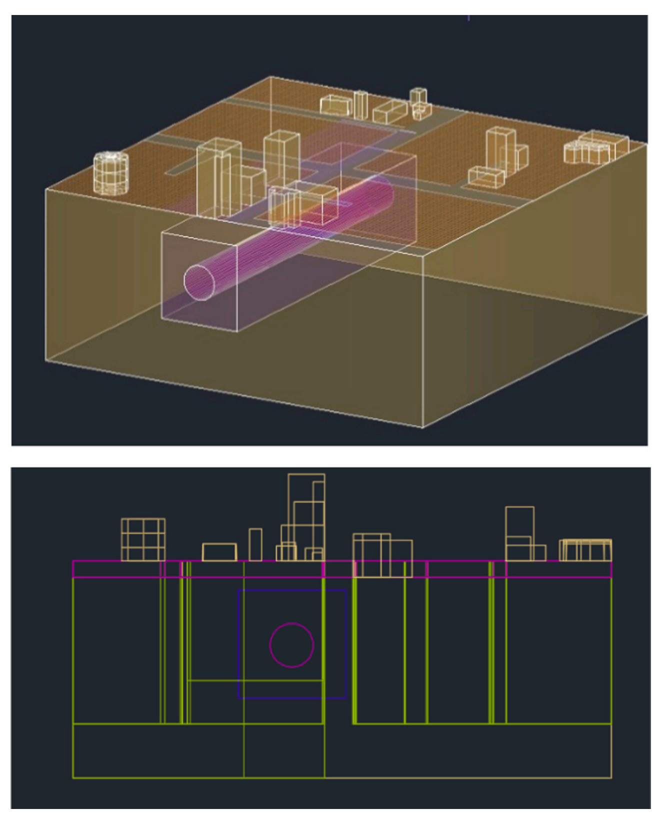

Fig. 11. Cadastral simulation: 3D model and planned tunnel route - perspective view (top), cross section view (bottom).

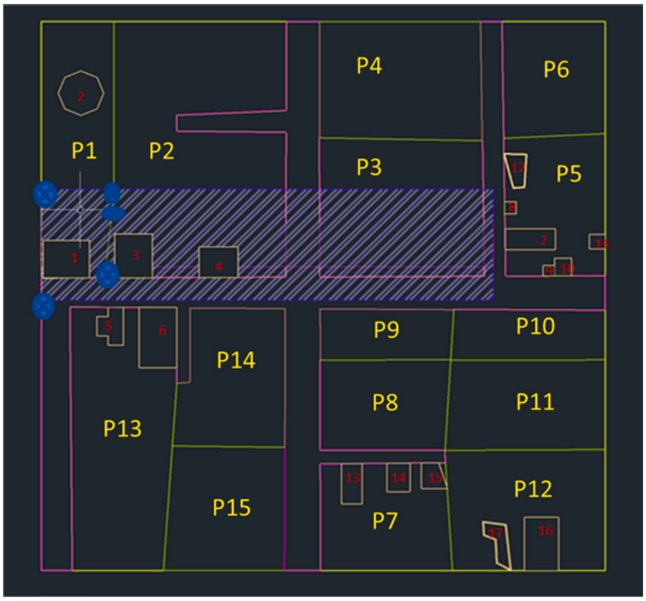

Fig. 12. Index of buildings (in red) and parcels (yellow, denoted with P). Railway tunnel is depicted in cyan. (For interpretation of the references to colour in this figure legend, the reader is referred to the web version of this article.)

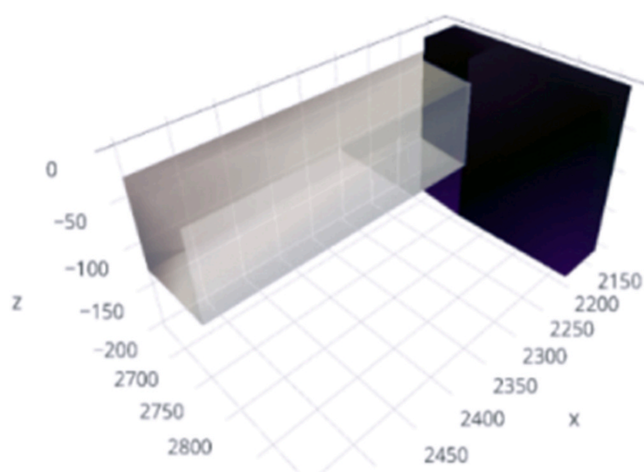

Fig. 13. The planned railway tunnel represented as a bounding box (grey) overlapping one of the 3DVPs (black).

including the whole air column above and below terrain, and 17 above terrain buildings (3DVPs), depicted in Fig. 12, limited by their co-ordinates. Since all buildings are above ground, their relationship with the tunnel will be evaluated in terms of their footprint.

Since the planned railway tunnel is cylindric, it is required to translate its geometry to a more simplified representation. Accordingly, we implemented two separate processes for evaluation: (1) creating a bounding box; and (2) surface approximation.

1. Bounding box: The planned railway tunnel was geometrically modified to a bounding box representation, depicted in Fig. 13 as a grey box. The bounding box is a depiction of a buffer around the tunnel, which in practice is required to keep a safe separation distance between the 3D objects. Using a buffer is a typical required regulation by many national cadastral institutions and is commonly done to handle inaccuracies associated with parcel surveying. The buffer represents the separation distance between buildings or underground utilities and may be implemented in underground buildings, railways, or railroads for reasons such as earthquake protection, fire escape and noise reduction. The bounding box comprises a buffer of 30 units in the direction of axis Y and Z, and 20 units in the direction of axis X.

The complete set of functions, outlined in Chapter 3, was implemented. The output, depicted in Table 2, accurately identified the spatial relationships of the 3DVPs and the planned railway tunnel: three 3DVPs were found to *overlap* with the tunnel, while the rest are *disjoint*. None of the buildings overlap the tunnel or its bounding box, though, the footprint of three buildings shows an *overlap* relationship with the tunnel. The bounding box defining the safe distance surrounding the tunnel partially falls under a road, which is a public tenure, meaning that no expropriation will be needed within the streets' volumes. Besides, the 3DVPs defining the streets are limited in their height coordinates - − 15.000–0.000 m, while the height of the bounding box ranges from − 26.438 m to − 126.438 m. Intersection coordinates required to produce the 3DVP were automatically generated, depicted in Fig. 14, and when compared to the intersection coordinates that were manually sampled in AutoCAD, all had identical coordinate values.

2. Surface approximation: the planned railway tunnel is presented by 8, 16 and 32 planar surfaces instead of cylindric shape. Fig. 15 (right) depicts the tunnel in its 8-planar approximation representation. The vertices in the cross-section view of the planned railway tunnel approximation (Fig. 15, left) are calculated based on the circle equation corresponding to the number of surfaces. The volume for each approximation (with coordinates $\{E_i, N_i\}$) is calculated according to the Simpson formula (see Eqs. (3) and (4)) and was

Table 2
Output relationships of the planned railway tunnel with the 2D parcels (left) and the (3DVP) buildings (right).

Parcel	Bottom Height	Relationship	Building	Top Height	Footprint Relationship
1	-200.000	*overlap*	1	79.999	*overlap*
2	-150.000	*overlap*	2	39.017	*disjoint*
3	-150.000	*overlap*	3	33.024	*overlap*
4	-150.000	*disjoint*	4	55.043	*overlap*
5	-150.000	*disjoint*	5	25.000	*disjoint*
6	-150.000	*disjoint*	6	18.970	*disjoint*
7	-150.000	*disjoint*	7	33.000	*disjoint*
8	-150.000	*disjoint*	8	30.000	*disjoint*
9	-150.000	*disjoint*	9	8.002	*disjoint*
10	-150.000	*disjoint*	10	12.302	*disjoint*
11	-150.000	*disjoint*	11	17.515	*disjoint*
12	-150.000	*disjoint*	12	16.234	*disjoint*
13	-150.000	*disjoint*	13	15.003	*disjoint*
14	-150.000	*disjoint*	14	50.000	*disjoint*
15	-150.000	*disjoint*	15	22.800	*disjoint*
			16	19.010	*disjoint*
			17	20.095	*disjoint*

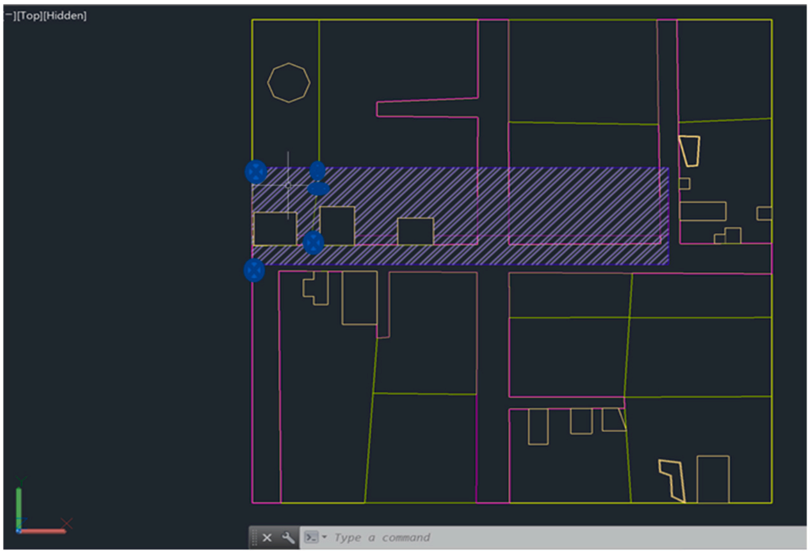

	X	Y	Z
1	2130.246	2685.834	-26.438
2	2130.246	2685.834	-126.438
3	2130.246	2766.168	-26.438
4	2130.246	2766.168	-126.438
5	2186.579	2686.071	-26.438
6	2186.579	2686.071	-126.438
7	2194.947	2760.822	-26.438
8	2194.947	2760.822	-126.438
9	2194.947	2766.168	-26.438
10	2194.947	2766.168	-126.438

Fig. 14. Top view of the automatically calculated intersection points (blue dots) of the planned railway tunnel bounding box and an *overlapping* parcel (left); automatically calculated intersection points coordinates (right). (For interpretation of the references to colour in this figure legend, the reader is referred to the web version of this article.)

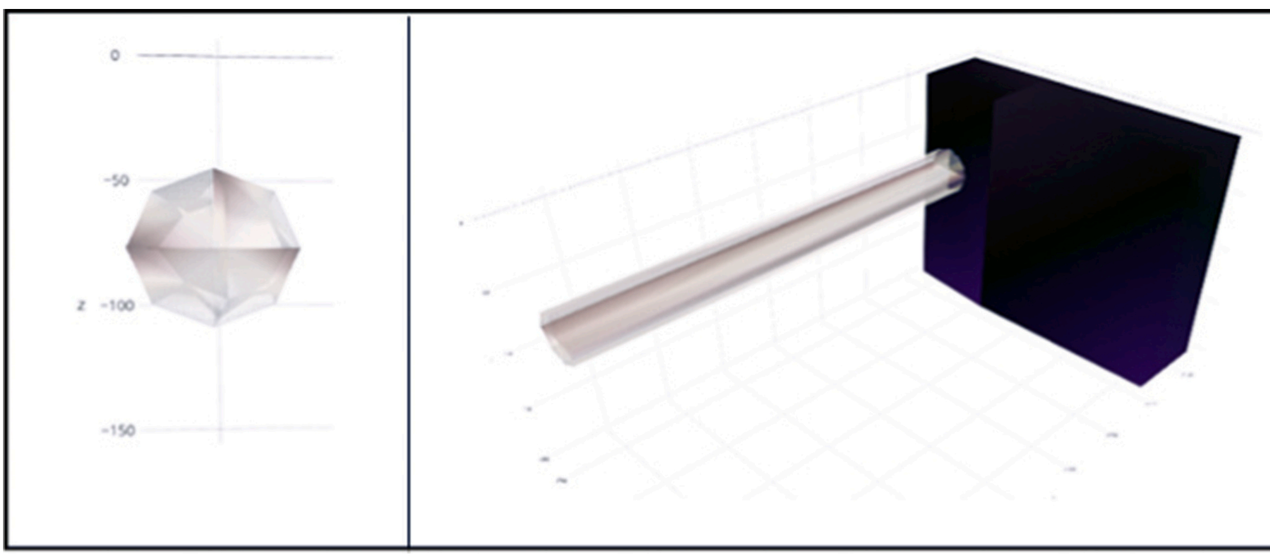

Fig. 15. The planned railway tunnel represented as eight plane surface approximation (grey) overlapping one of the 3D volumetric parcels (black).

Table 3
Volume values planned for expropriation from parcel 1 according to the three tunnel approximations implemented in the simulation.

Approximation	Calculated volume (m^3)	Volume difference (m^3)	Difference percentage (%)	Ratio between differences
Circle (none)	1256.637	–	–	–
8-planes	1131.371	125.266	9.97	–
16-planes	1224.587	32.050	2.55	0.26
32-planes	1254.619	2.018	0.16	0.06

compared to the precise original surface (circle area), depicted in Table 3. These results show that there is an importance to choosing the approximation method.

$$CrossSection \quad Area = \frac{1}{2}\left|\sum\nolimits_{i=1}^{n} N_i \cdot (E_{i+1} - E_{i-1})\right| \tag{3}$$

$$V = \frac{L}{6}[A_1 + 4A_m + A_2], where\ A_1 = A_2 = A_m \tag{4}$$

Similar relationships were retrieved for the surface approximation (as in Table 2), correctly identifying the relationship types, and accurately extracting the coordinate values of the intersection points, which were the same as the ones manually sampled in AutoCAD. Since three approximations were used, different intersection points and hence expropriated volume values are calculated, depicted in Table 3. The volume values are required to calculate the compensation costs, which are necessary for measuring economic effectiveness of the planned tunnel route and making decisions. Moreover, intersection points enable subdividing the parcel and creating two sub-parcels describing the expropriated fraction and the remainder fraction.

5. Discussion and Conclusions

The implementation of 3D cadastres has been under discussion among academics as well as practitioners and cadastral authorities for over a decade. The urge for expanding the projection of rights, restrictions, and responsibilities from 2D projection into actual 3D is understandable; the recent megatrend of urbanization and demographic changes put pressure on cities to expand upwards and downwards. The trend of densification by increasing the volume of built-up properties by expanding in 3D, and utilizing infill development where possible, causes the urban land value to rise. And the more valuable land is, the more attention should be paid to precisely defined three Rs (e.g., Krigsholm et al., 2020). The issue of rising land value and defining the extent of different interests in land is not only accelerator to implement 3D cadastre. Urban development calls for more efficient use of urban space, including underground space. The underground space is used for parking, (railway) tunnels, and other urban infrastructure. Defining 3D land rights is essential in forming these spaces. The different interests in land are typically overlapping – same property is the object of several interests (Blandy et al., 2006; Niukkanen, 2014). When building new 3D urban infrastructure, these interests need to be clearly defined not only in respect to the existing property, but also in relation to other, surrounding properties.

In previous studies, the starting point for defining the topology of 3D objects has been the assumption that overlapping interests do not exist. Thus, they have been focused on simple cases with no overlaps and hollow objects. This study showed one solution for modeling the complex topology of the 3D objects and overlapping interests, to implement a 3D cadastre. The study shows that our solution is useful in cases where there are complex parcels and complex interests, which is the case typically in urban development. The developed algorithms can be used in typical complex cases, but to validate its universal applicability, more case studies should be conducted.

This paper aimed at setting practical analytical steps for determining the topology between 3DVPs. While existing algorithms are applicable for simple parcels - although in some cases limited, in this work we aimed to extend this to complex parcels, as is the common case for 3DVPs stored in land administration systems. Namely, we focused on parcels that are partially unbounded, concave, or hollowed, and have non-parallel roof/floor. For that, we suggested a hierarchical definition of 3DVPs, developing steps to handle the above. In addition, we define a subdivision function for concave and hollowed 3DVPs.

Results for several examples and simulations that replicate real case studies involving complex 3DVPs were found to be accurate by correctly identifying the spatial relationships and coordinates of, e.g., intersection points. While previous algorithms failed to accurately detect spatial relationships due to their limitation in identifying intersection points between concave parcels, we were able to achieve that using the subdivision algorithm. As far as we know, this is the first attempt that suggests an algorithm for subdividing 3D concave parcels into convex ones. However, the algorithm has few shortcomings, such as the necessity to insert coordinates, edges, and faces (that define the 3DVP) in a specific uniform order. Alongside the requirement to define each edge twice (in two opposite directions) since an edge is a border of two faces. Neither the approximations of curved surfaces, nor the coordinates of parcels in real databases, can be absolutely precise in terms of their measured position (coordinates), which leads to inaccurate representation of the formulas defining edges and surfaces of parcels. This requires using a tolerance interval while implementing the mathematical functions (see Appendix B and C) for avoiding producing incorrect conclusions.

The hierarchical definition of 3DVPs (parcel, face, edge, point) enables the implementation of additional 3D functionalities (e.g., creating a 3D buffer, volume calculation, subdivision), which may further facilitate applying a complete 3D cadastral process. The proposed data structure for this algorithm can be conceived as an extended 2D data structure, e.g., expanding existing 2D cadastral systems, and handling 2D objects as a private instance of a 3D object while using a Boolean field for indicating whether a specific object is planar or spatial. For the proposed algorithms, using python programming language is recommended, since Python allows reading DXF files, which may allow linking cadastral functionalities to cadastral CAD files. It also enables scripting into programs that handle 3D entities, such as: ESRI's CityEngine and ArcGIS Pro. In addition, Python contains extensive support libraries that can be used for computation, creating GUIs, or plotting.

In future research, accuracy-related questions should be discussed, such as: should the thickness of a plane be taken in consideration (i.e., the building walls are not planar but 3-dimensional ones)? What is the practical accuracy of storing cadastral data and coordinates into databases? Besides, does a vertex have to lay exactly on a plane for inducing that it touches it? In which cases a threshold should be allowed and according to which criteria should it be determined? Answers for these questions varies depending on different land registration systems and should be locally answered. In this study, the algorithms were tested for small-scale experiments, such that computational topology challenges and optimization will be investigated to ensure the handling of large-scale projects with numerous 3D parcels to ensure scalability by adapting methods as octree-based mesh and parallel computing. Methods will also include automatic pre-processing solutions for inputting coordinates counterclockwise.

Solving 3D topological problems might be imbedded in basic practical procedures essential for further implementations like digital twins, which is being advanced by several countries (e.g., Tao and Qi, 2019), including the use of virtual reality (VR), as well as sustainable multi-purpose, multi-dimensional land management systems (Jaljolie and Dalyot, 2019, 2020). These examples depict the spatial reality and manage of 3D land resources, meaning that 3D algorithms, procedures, and functionalities, such as those provided in our paper, are supposed to contribute towards their development and implementation.

The rather strong division in research of 3D land administration between the legal and institutional questions and aspects, and technical issues such as topology, reflects the situation in academy and cadastral authorities alike. The expertise is divided between these groups, leaving the common understanding and discussion of the holistic view on land administration with all its dimensions lacking. This article contributes to the combination of technical and institutional knowledge in the field of land administration, striving towards the common goal of implementing 3D cadastre.

Appendix A. Supporting information

Supplementary data associated with this article can be found in the online version at doi:10.1016/j.landusepol.2021.105637.

References

Blandy, S., Dixon, J., Dupuis, A., 2006. Theorising power relationships in multi-owned residential developments: unpacking the bundle of rights. Urban Stud. 43 (13), 2365–2383.

Bozickovic, Z., Dzelalija, G., Ivanovic, A., 2012. Topological operations on simple three dimensional objects in geoinformation systems. Counc. Eur. Geod. Surv.

Bureick, J., Neuner, H., Harmening, C., Neumann, I., 2016. Curve and surface approximation of 3D point clouds. Allg. Vermess. Nachr. 123 (11–12), 315–327.

Chen, T.K., Abdul-Rahmana, A., Zlatanova, S., 2008. 3D spatial operations for geo-DBMS: geometry vs. topology. The International Archives of the Photogrammetry. Remote Sens. Spat. Inf. Sci. 37 (B2), 549–554.

Congli, W., Tsuzuki, M.D.S.G., 2004. Representation of curves and surfaces in b-rep solid modelers. ABCM Symp. Mechatron. 1, 498–507.

Dimopoulou, E., Van Oosterom, P. (Eds.), 2019. Research and Development Progress in 3D Cadastral Systems. MDPI.

Doulamis, A., Soile, S., Doulamis, N., Chrisouli, C., Grammalidis, N., Dimitropoulos, K.,. & Ioannidis, C. (2015, June). Selective 4D modelling framework for spatial-temporal land information management system. In Third International Conference on Remote Sensing and Geoinformation of the Environment (RSCy2015) (Vol. 9535, p. 953506). International Society for Optics and Photonics.

Egenhofer, M.J., Franzosa, R.D., 1991. Point-set topological spatial relations. Int. J. Geogr. Inf. Syst. 5 (2), 161–174.

Ericson, C., 2004. Real-Time Collision Detection. CRC Press.

Granados, M., Hachenberger, P., Hert, S., Kettner, L., Mehlhorn, K., Seel, M., 2003. Boolean operations on 3D selective Nef complexes: data structure, algorithms, and implementation. European Symposium on Algorithms. Springer, Berlin, Heidelberg, pp. 654–666.

Hmida, H. B., Cruz, C., Boochs, F., & Nicolle, C. (2013). From 9-IM topological operators to qualitative spatial relations using 3D selective Nef complexes and logic rules for bodies. arXiv preprint arXiv:1301.4992.
Hoppenbrouwer, E., Louw, E., 2005. Mixed-use development: theory and practice in Amsterdam's Eastern Docklands. Eur. Plan. Stud. 13 (7), 967–983.
Jaljolie, R., Dalyot, S., 2019. Formalizing a multi-dimensional land management system: the Stakeholders' perspective. Int. Arch. Photogramm. Remote Sens. Spat. Inf. Sci. XLII-4/W15, 27–33.
Jaljolie, R., Dalyot, S., 2020. Multi-dimensional land management systems: a delphi study of the expert community. FIG Work. Week.
Jaljolie, R., van Oosterom, P.J. M., & Dalyot, S. (2016). Systematic analysis of functionalities for the Israeli 3D cadastre. In 5th International Fig. 3D Cadastre Workshop. International Federation of Surveyors (FIG).
Jaljolie, R., Van Oosterom, P., Dalyot, S., 2018. Spatial data structure and functionalities for 3D land management system implementation: Israel case study. ISPRS Int. J. Geo Inf. 7 (1), 10.
Kalogianni, E., van Oosteom, P., Dimopoulou, E., Lemmen, C., 2020. 3D land administration: a review and a future vision in the context of the spatial development lifecycle. ISPRS Int. J. Geo Inf. 9 (2), 107.
Kang, H., Lee, J., 2014. A study on the LOD (Level of Detail) model for applications based on indoor space data. J. Korean Soc. Surv. Geod. Photogramm. Cartogr. 32 (2), 143–151.
Karki, S., Thompson, R., McDougall, K., 2013. Development of validation rules to support digital lodgement of 3D cadastral plans. Comput. Environ. Urban Syst. 40, 34–45.
Kemec, S., Zlatanova, S., & Duzgun, S. (2012). A new LoD definition hierarchy for 3D city models used for natural disaster risk communication tool. In Proceedings of the 4th International Conference on Cartography & GIS, Volume 2, Albena, June 2012, pp. 17–28. International Cartographic Association.
Krigsholm, P., Riekkinen, K., Ståhle, P., 2018. The changing uses of cadastral information: a user-driven case study. Land 7 (3), 83.
Krigsholm, P., Riekkinen, K., Ståhle, P., 2020. Pathways for a future cadastral system: a socio-technical approach. Land Use Policy 94, 104504.
Kusumastuti, D., Nicholson, A., 2018. Mixed-use development in Christchurch, New Zealand: do you want to live there? Urban Stud. 55 (12), 2682–2702.
Luo, W., Hu, Y., Yu, Z., Yuan, L., Lü, G., 2017a. A hierarchical representation and computation scheme of arbitrary-dimensional geometrical primitives based on CGA. Adv. Appl. Clifford Algebras 27 (3), 1977–1995.
Luo, W., Yu, Z., Yuan, L., Hu, Y., Zhu, A.X., Lü, G., 2017b. Template-based GIS computation: a geometric algebra approach. Int. J. Geogr. Inf. Sci. 31 (10), 2045–2067.
Mualam, N., Salinger, E., Max, D., 2019. Increasing the urban mix through vertical allocations: public floorspace in mixed use development. Cities 87, 131–141.
Niukkanen, K. 2014. On the property rights in Finland – the point of view of legal cadastral domain model. Doctoral dissertation, Aalto University.
Pigot S. 1991 Topological models for 3D spatial information systems. In Proceedings of Autocarto 10, Baltimore, Maryland: 368–392.
Schwanke, D., 2005. Mixed-use Development Handbook. Urban Land Institute, Washington D.C.
Seifert, M., Gruber, U., Riecken, J., 2017. Germany on the Way to 4D-Cadastre. Cadastre: Geo-Information Innovations in Land Administration. Springer, Cham, pp. 147–158.
Shi, Z., Hu, D., Yin, P., Wang, C., Chen, T., Zhang, J., 2019. Calculation for multidimensional topological relations in 3D cadastre based on geometric Algebra. ISPRS Int. J. Geo Inf. 8 (11), 469.
Shojaei, D., Olfat, H., Faundez, S.I.Q., Kalantari, M., Rajabifard, A., Briffa, M., 2017. Geometrical data validation in 3D digital cadastre– a case study for Victoria, Australia. Land Use Policy 68, 638–648.
Siemiatycki, M., 2015. Mixing public and private uses in the same building: opportunities and barriers. J. Urban Des. 20 (2), 230–250.
Tao, F., Qi, Q., 2019. Make more digital twins. Nature 573, 490–491.
Thompson, R.J., van Oosterom, P., 2011. Integrated representation of (potentially unbounded) 2D and 3D spatial objects for rigorously correct query and manipulation. Advances in 3D Geo-Information Sciences. Springer, Berlin, Heidelberg, pp. 179–196.
Ting, L., Williamson, I., 1999. Cadastral trends: a synthesis. Aust. Surv. 44 (1), 40–54.
van Oosterom, P., 2013. Research and development in 3D cadastres. Comput. Environ. Urban Syst. 40, 1–6.
Van Oosterom, P.J. M. (2018). Best practices 3D cadastres–extended version international federation of surveyors. Copenhagen, Denmark, March.
Ying, S., Guo, R., Li, L., Van Oosterom, P., Stoter, J., 2015. Construction of 3D volumetric objects for a 3D cadastral system. Trans. GIS 19 (5), 758–779.
Yu, Z., Luo, W., Yuan, L., Hu, Y., Zhu, A.X., Lü, G., 2016. Geometric algebra model for geometry-oriented topological relation computation. Trans. GIS 20 (2), 259–279.
Zhang, J.Y., Yin, P.C., Li, G., Gu, H.H., Zhao, H., Fu, J.C., 2016. 3D cadastral data model based on conformal geometry algebra. ISPRS Int. J. Geo Inf. 5 (2), 20.
Zomorodian, A., & Edelsbrunner, H. (2000, May). Fast software for box intersections. In Proceedings of the sixteenth annual symposium on Computational geometry (pp. 129–138).